Cell Research (2008) 18:1020-1036.

www.nature.com/cr

ORIGINAL ARTICLE

BCL-X_L regulates TNF-α-mediated cell death independently of NF-κB, FLIP and IAPs

Raffaella Gozzelino[1], Carme Sole[1], Nuria Llecha[2], Miguel F Segura[1], Rana S Moubarak[3], Victoria Iglesias-Guimarais[3], M Jose Perez-Garcia[1], Stephanie Reix[3, 4], Jisheng Zhang[1], Nahuai Badiola[3, 4], Daniel Sanchis[1], Jose Rodriguez-Alvarez[3, 4], Ramon Trullas[5], Victor J Yuste[3, *], Joan X Comella[1, 3, 4, *]

[1]Cell Signaling and Apoptosis Group, Departament de Ciències Mèdiques Bàsiques, Universitat de Lleida, Montserrat Roig, 2, 25008 Lleida, Spain; [2]Departament de Patologia i Genètica Molecular, Hospital Universitari Arnau de Vilanova, Universitat de Lleida, Montserrat Roig, 2, 25008 Lleida, Spain; [3]Institut de Neurociències, Departament de Bioquímica i Biologia Molecular, Facultat de Medicina, Universitat Autònoma de Barcelona, Campus de Bellaterra (Edifici M), 08193 Bellaterra, Spain; [4]Centro de Investigación Biomédica en Red sobre Enfermedades Neurodegenerativas (CIBERNED), Spain; [5]Neurobiology Unit, Institut d'Investigacions Biomèdiques de Barcelona, CSIC, IDIBAPS, 08036 Barcelona, Spain

Upon activation, tumor necrosis factor alpha (TNF-α) receptor can engage apoptotic or survival pathways. Inhibition of macromolecular synthesis is known to sensitize cells to TNF-α-induced cell death. It is believed that this sensitization is due to the transcriptional blockade of genes regulated by NF-κB. Nevertheless, such evidence has remained elusive in the nervous system. Here, we show that TNF-α cannot normally induce apoptosis in PC12 cells or cortical neurons. However, cells treated with Actinomycin D (ActD) become susceptible to TNF-α-induced cell death through the activation of caspase-8, generation of tBid and activation of caspase-9 and -3. Analysis of several proteins involved in TNF-α receptor signaling showed no significant downregulation of NF-κB target genes, such as IAPs or FLIP, under such conditions. However, Bcl-x_L protein levels, but not those of Bcl-2, Bax and Bak, are reduced by ActD or TNF-α/ActD treatments. Moreover, Bcl-x_L overexpression fully protects cells against TNF-α/ActD-induced cell death. When endogenous levels of Bcl-x_L are specifically downregulated by lentiviral-based RNAi, cells no longer require ActD to be sensitive to TNF-α-triggered apoptosis. Furthermore, Bcl-x_L downregulation does not affect TNF-α-mediated NF-κB activation. Altogether, our results demonstrate that Bcl-x_L, and not Bcl-2, FLIP or IAPs, acts as the endogenous regulator of neuronal resistance/sensitivity to TNF-α-induced apoptosis in an NF-κB-independent manner.

***Keywords*:** apoptosis, Bcl-x_L, neuron, NF-κB, PC12, TNF-α

Cell Research (2008) **18**:1020-1036. doi: 10.1038/cr.2008.76; published online 1 July 2008

Introduction

Tumor necrosis factor alpha (TNF-α) is widely expressed in most tissues, including the nervous system. Under normal conditions, TNF-α is expressed at low levels in neurons in the Central Nervous System (CNS) [1]. However, its expression increases drastically after different pathological stimuli such as neural injury, ischemia or infection. The main source of TNF-α is the resident glia that becomes activated as part of the innate inflammatory response of the CNS [2]. TNF-α appears to be one of the most important mediators of the deleterious effects observed in several pathologies in the nervous system such as axotomy [3], Parkinson- [4, 5] or stroke-induced damage [6] and spinal cord injury [7].

TNF-α can induce either cell death or cell survival and proliferation [8]. When TNF-α binds to its receptor TNFR1, an NF-κB-activating complex (complex I), composed of TRADD, RIPK and TRAF2, is formed [9]. Subsequently, TRADD dissociates from the receptor and recruits FADD and caspase-8, forming complex II. TNF-α induces cell survival in cells that strongly activate NF-κB, whereas apoptosis occurs when NF-κB is poorly activated. Therefore, it is well established that TNF-α-induced apoptosis requires simultaneous NF-κB inhibition [10-12]. Inhibition

*These two authors are co-senior authors to this work.
Correspondence: Victor J Yuste
Tel: +34-9-35-81-37-62; Fax: +34-9-35-81-15-73
E-mail: victor.yuste@uab.cat
Received 2 February 2008; revised 15 April 2008; accepted 25 April 2008; published online 1 July 2008

of NF-κB can be achieved by blocking RNA or protein synthesis using Actinomycin D (ActD) or cycloheximide (CHX), respectively [13-15]. However, these experimental approaches are not specific for NF-κB, making the results difficult to interpret. Several NF-κB target genes such as c-FLIP$_L$, c-IAP1/2 and XIAP have been proposed to play protective roles, inhibiting apoptosis via different mechanisms. Several reports have shown that ActD and CHX also reduce c-FLIP$_L$ and c-IAP levels [14, 15]. Bcl-2, Bcl-x$_L$ or Mcl-1 overexpression has also been shown to protect cells from TNF-α-induced cell death [16-19]. Nonetheless, there are no conclusive reports concerning the relevance of these proteins as endogenous inhibitors of TNFR-triggered apoptosis.

Here, we demonstrate that Bcl-x$_L$ levels are a crucial determinant of resistance or sensitivity to TNF-α-induced cell death in neurons. TNF-α can only induce apoptosis in PC12 cells or cortical neurons when macromolecular synthesis is blocked. In these cells, ActD specifically downregulates Bcl-x$_L$ without affecting FLIP or IAP levels. We also show that inhibiting NF-κB does not modify Bcl-x$_L$ levels. When endogenous Bcl-x$_L$ levels are downregulated by RNAi, TNF-α can induce apoptosis without the further requirement of ActD and despite the simultaneous activation of the NF-κB pathway. Together, our results suggest that Bcl-x$_L$ is part of an NF-κB-independent pathway that protects cells from TNF-α-induced apoptosis.

Results

Inhibition of macromolecular synthesis renders PC12 cells and primary cortical neurons sensitive to the cytotoxic activity of TNF-α

It is well-documented that some cell types are resistant to the cytotoxic effects of TNF-α. However, many cell types become sensitive to TNF-α when cells are treated with ActD to inhibit RNA synthesis [10, 11]. The molecular mechanisms underlying this phenomenon remain poorly understood. As shown in Figure 1A, the addition of TNF-α did not impair the normal proliferation rate of PC12 cells compared with their untreated controls. To render them sensitive to TNF-α-induced cytotoxicity, cells were treated with TNF-α in the presence of 1 nM ActD. After 24 h, approximately 20% of the cells died (Figure 1B). Hoechst staining revealed that most of the dying cells displayed a typical apoptotic nuclear morphology characterized by chromatin condensation and shrinkage of the nucleus (Figure 1B). Apoptotic nuclear characteristics were further confirmed by TUNEL assay (Figure 1B). However, the addition of neither ActD nor TNF-α alone had any effects on cell viability (Figure 1A and 1B), although ActD impaired the proliferation of PC12 cells (Figure 1A). Co-treatment with TNF-α and ActD (TNF-α/ActD) induced a nearly 3-fold increase in caspase-8-like (IETDase) activity compared to untreated PC12 cells or PC12 cells treated with ActD or TNF-α alone. When 50 μM z-IETD-fmk was included in the culture media, caspase-8-like activation was completely prevented (Figure 1C). In addition, the processing of Bid into its caspase-8-specific truncated form, tBid, occurred only when cells were co-treated with TNF-α/ActD (Figure 1D). Figure 1D demonstrates the involvement of the intrinsic apoptotic pathway through the processing of pro-caspase-9 into its p38 and p17 active fragments and pro-caspase-3 into its large p17 active form. Activation of caspase-3 was confirmed by measuring DEVDase activity (Figure 1E). This activity, as well as the resulting apoptosis, could be fully inhibited by z-VAD-fmk (Figure 1E and data not shown).

Results similar to those described for PC12 cells were also obtained using primary neurons. Embryonic cortical neurons were resistant to TNF-α-induced apoptosis, but co-treatment with TNF-α/ActD induced a significant increase in cell death ($P < 0.01$), as well as the processing and activation of procaspase-9 and procaspase-3 (Figure 1F). We also observed that neurons treated with TNF-α/ActD displayed caspase-8-like and caspase-3-like activities as assessed by measuring their enzymatic activities using the fluorogenic substrates IETD-afc and DEVD-afc, respectively (Figure 1G and 1H).

Inhibition of macromolecular synthesis does not modify the levels of death-inducing signaling complex (DISC) adaptors or inhibitors

ActD-mediated sensitization to TNF-α-induced cell death could be due to an imbalance between the "survival complex" (integrated by TNF-α/TNF-R1/TRADD/TRAF-2/RIPK) and the "death complex" (formed by TNF-α/TNF-R1/TRADD/FADD) [8]. To ascertain whether ActD modifies the levels of the molecular adaptors mentioned above, we generated western blots of PC12 cell lysates using specific antibodies against TNF-R1, TRADD, FADD, TRAF-2 and RIPK. As shown in Figure 2A, none of these proteins displayed significant changes after treatment with TNF-α, ActD or TNF-α/ActD. Since there are no good antibodies against the rat variants of TNF-R2 and caspase-8, we also checked the expression of their miRNAs by semi-quantitative RT-PCR. Whereas TNF-R1 was present in PC12 cells (Figure 2A), we failed to detect TNF-R2 transcripts (Figure 2B and [20]). Caspase-8 mRNA levels remained unaltered by the experimental treatments (Figure 2B). As observed in PC12 cells, ActD did not modify levels of DISC components in primary cortical neurons (Figure 2A and 2B).

FLIP$_L$ and IAP levels have been proposed to be critical

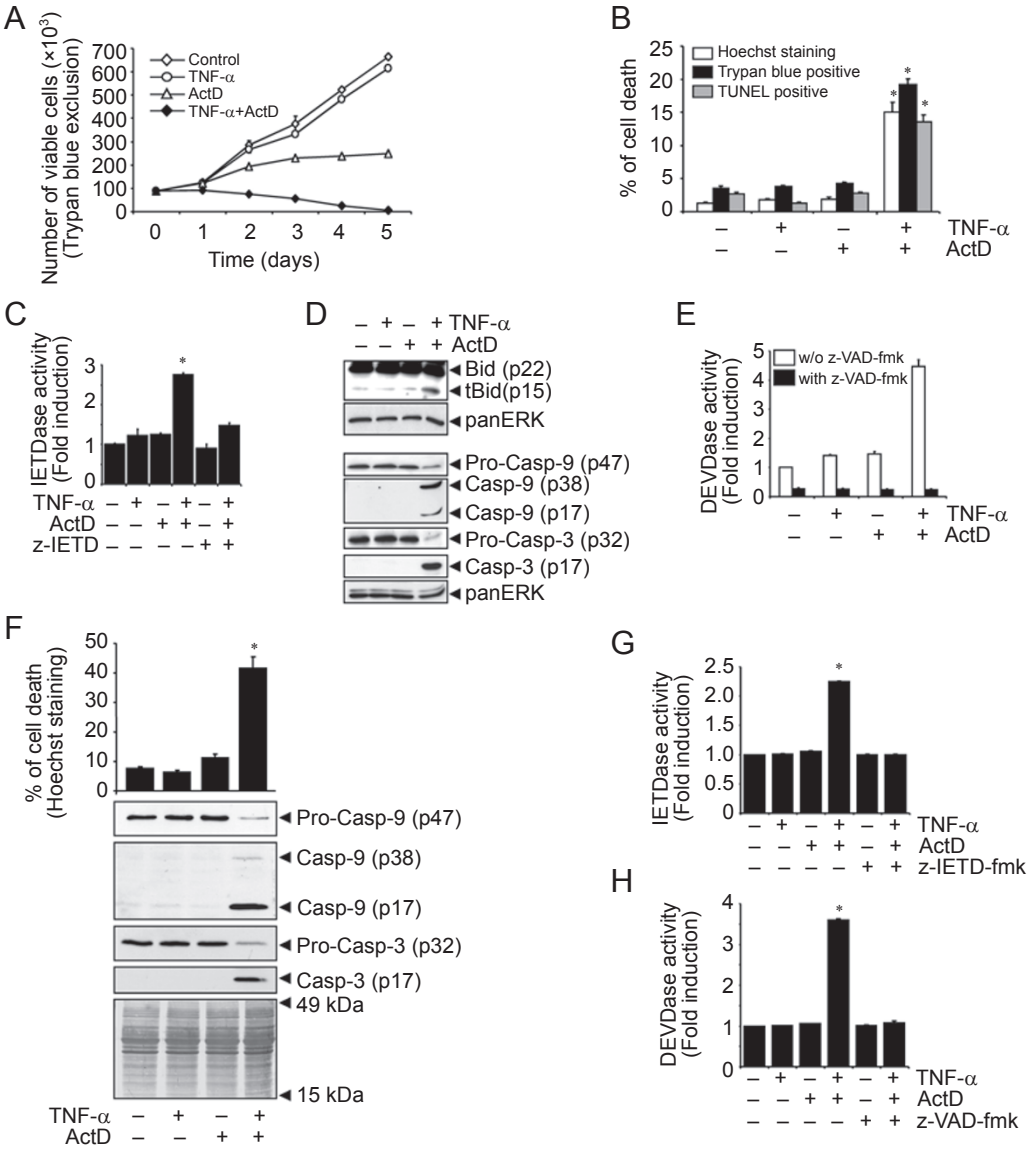

Figure 1 PC12 cells are resistant to TNF-α-induced cell death, but become sensitive after treatment with actinomycin D (ActD). **(A)** PC12 cells were maintained in culture for the indicated times and experimental conditions, and cell proliferation was estimated by Trypan blue exclusion. Note the exponential growth of control or TNF-α-treated cells, whereas those treated with ActD cease growing but do not die. All cells co-treated with TNF-α and ActD die after 5 days of treatment. **(B)** PC12 cells were left untreated or treated with 100 ng/ml TNF-α and/or 1 nM ActD for 24 h. Cell death was quantified by Trypan blue exclusion assay (black columns), counting apoptotic nuclear morphology using Hoechst 33258 staining (white columns) or by the TUNEL technique (grey columns). **(C)** Caspase-8 activity was measured after 8 h of treatment using the fluorogenic Ac-IETD-afc reagent. Addition of 50 μM z-IETD-fmk (a caspase-8 inhibitor) was used to verify caspase-8 involvement. **(D)** Total lysates from cells treated for 24 h were analyzed by western blot to detect the caspase-8 specific processing of Bid (p22) by the appearance of the truncated fragment (tBid p15) (upper panels). Moreover, caspase-9 and -3 activations were determined by the detection of the cleaved forms of p38 and p17 for caspase-9 and p17 for caspase-3 (lower panels). Loading controls were performed by probing the membrane with an anti-panERK antibody. **(E)** Caspase-3-like activity was measured using the fluorogenic Ac-DEVD-afc reagent after 8 h of the indicated treatments without (white columns) or with (black columns) 50 μM of the general caspase inhibitor z-VAD-fmk. **(F-H)** Primary mouse cortical neurons were maintained for 6 days *in vitro* (DIV), then treated with TNF-α and/or ActD for 24 h. **(F)** Cell death was quantified by counting apoptotic nuclei after Hoechst 33258 staining. Caspase-9 and caspase-3 activation was detected only after TNF-α/ActD treatment by means of the appearance of the activation-specific fragments (lower panels). Naphtol blue (NB) staining was used to control for membrane protein content. **(G, H)** Caspase-8-like and caspase-3-like activities were measured after 8 h of treatment using the fluorogenic Ac-IETD-afc or Ac-DEVD-afc reagents, respectively. The specificity of the activity was assessed by the addition of 50 μM of the caspase-8 inhibitor z-IETD-fmk or 50 μM of the general caspase inhibitor z-VAD-fmk during the treatments. *$P < 0.01$.

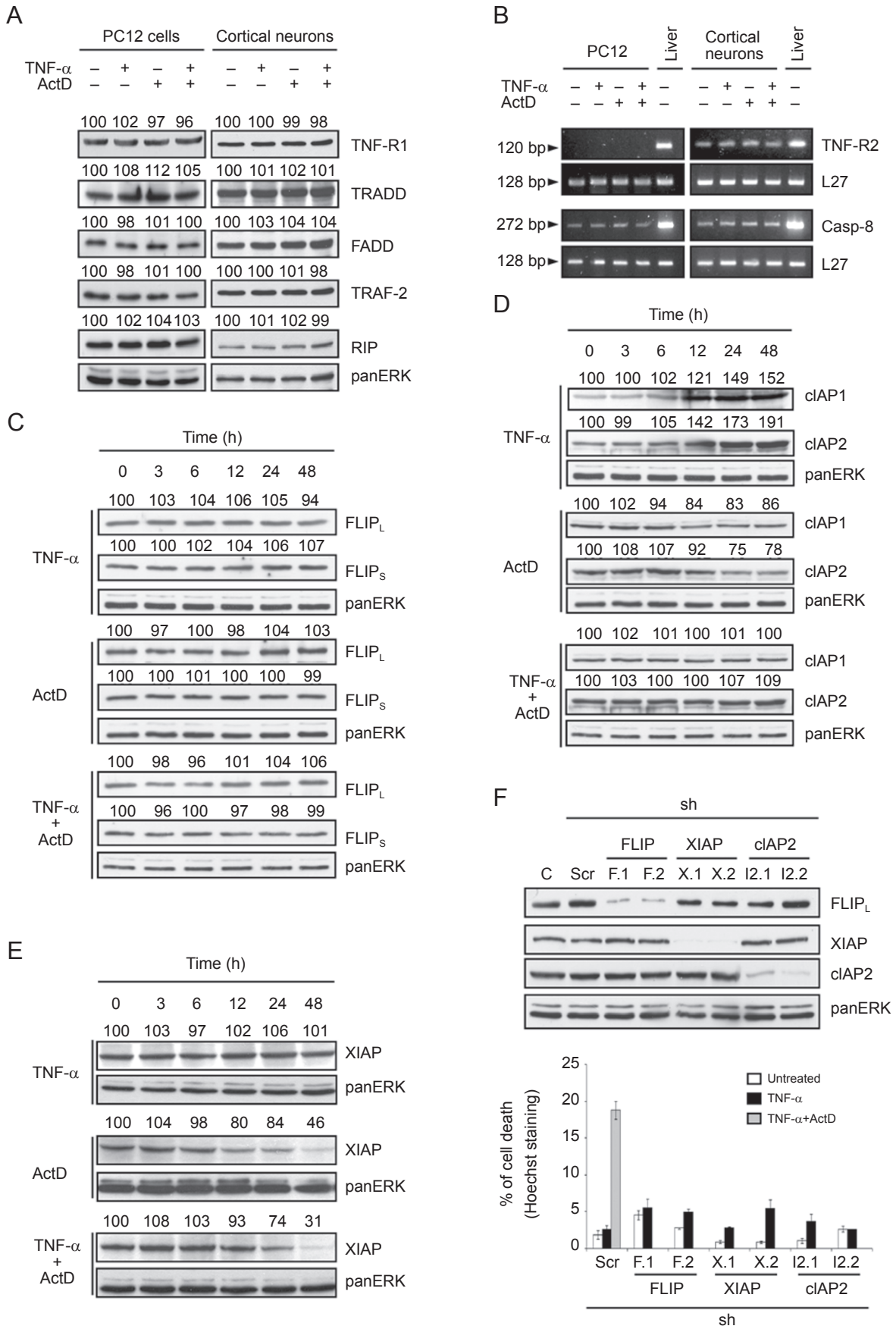
A
PC12 cells
Cortical neurons
TNF-α
ActD
TNF-R1
TRADD
FADD
TRAF-2
RIP
panERK
B
PC12
Liver
Cortical neurons
Liver
120 bp
128 bp
272 bp
TNF-R2
L27
Casp-8
C
Time (h)
TNF-α
ActD
FLIP$_L$
FLIP$_S$
panERK
D
Time (h)
cIAP1
cIAP2
panERK
E
XIAP
F
sh
FLIP
XIAP
cIAP2
C
Scr
F.1
F.2
X.1
X.2
I2.1
I2.2
% of cell death (Hoechst staining)
Untreated
TNF-α
TNF-α+ActD

for regulating sensitivity to or resistance against TNF-α in several cellular models [21, 22]. Both cIAP1 and cIAP2, but not FLIP or XIAP, levels increased upon TNF-α treatment in a time-dependent manner in PC12 cells (Figure 2C-2E). In addition, cIAP1, cIAP2 and XIAP protein levels decreased upon treatment with ActD, but those of FLIP remained unaltered. Co-treatment with TNF-α and ActD did not cause significant changes in cIAP1, cIAP2 and $FLIP_L$ levels (Figure 2C and 2D), but caused a decrease in XIAP protein levels (Figure 2E). To ascertain whether decreased levels of some of these proteins could sensitize PC12 cells to TNF-α-induced cell death, we performed RNAi experiments. As shown in Figure 2F, knock-down of c-FLIP, XIAP or cIAP2 did not influence cell sensitivity to TNF-α. Together, these results suggest that the critical regulatory step is downstream of the DISC.

Inhibition of macromolecular synthesis decreases Bcl-x_L protein levels

Since Bcl-2 family members modulate cell death signals by affecting mitochondrial integrity, we wanted to know whether ActD treatment affects the levels of the anti-apoptotic proteins Bcl-2 and Bcl-x_L or the pro-apoptotic proteins Bax and Bak. Although untreated PC12 cells did not express Bcl-2 (data not shown and [23]), the other three proteins were present in untreated PC12 cells (Figure 3A). Treatment with TNF-α for 12, 24 or 48 h did not modify Bcl-x_L, Bax or Bak protein levels. However, treatment of PC12 cells with 1 nM ActD downregulated Bcl-x_L without altering Bax or Bak protein levels (Figure 3A). Bcl-x_L levels also decreased without any evident changes in Bax or Bak levels in cortical neurons after ActD treatment (Figure 3B). Unlike PC12 cells, cortical neurons express Bcl-2, but the expression of Bcl-2 was not affected by ActD treatment. In a more detailed time-course, we observed that Bcl-x_L levels diminished between 6 and 12 h after ActD treatment in PC12 cells (Figure 3C). A maximal decrease in Bcl-x_L expression was achieved after 48 h when the protein level was 40% lower than that observed in control cells (Figure 3C). To determine whether TNF-α/ActD-induced cell death correlated with the decrease in Bcl-x_L levels, we quantified apoptosis by assessing apoptotic nuclear morphology by Hoechst staining after 6, 12, 24 and 48 h of treatment. As shown in Figure 3D, PC12 cells became sensitive to apoptosis between 12 and 24 h after TNF-α/ActD co-treatment. These results indicate that RNA synthesis inhibition by ActD induces a decrease in Bcl-x_L protein levels that precedes sensitization to TNF-α-induced cell death.

Overexpression of Bcl-x_L blocks TNF-α/ActD-induced cell death in PC12 cells and cortical neurons

To confirm that Bcl-x_L confers resistance against TNF-α/ActD-induced apoptosis, PC12 cells were infected with a lentivirus carrying a eukaryotic expression construct containing the human *bcl-x_L* gene (PC12-Bcl-x_L). After 72 h of infection, cells were treated with ActD and Bcl-x_L expression levels were monitored. As shown in Figure 4A, at the beginning of ActD treatment (72 h post-infection), PC12 cells infected with the Bcl-x_L construct expressed nearly twice as much Bcl-x_L as cells infected with an empty vector. ActD treatment induced a progressive decrease in Bcl-x_L levels in both control and Bcl-x_L-infected cells (Figure 4A). However, even after 24 h of ActD treatment, PC12-Bcl-x_L cells maintained Bcl-x_L expression levels that were higher than empty vector-infected PC12 cells (Figure 4A). In agreement with the results described above, Bcl-x_L overexpressing cells were resistant to death induced by TNF-α/ActD treatment. Bcl-x_L overexpression was as ef-

Figure 2 Inhibition of RNA synthesis does not affect the expression levels of the DISC components, IAPs or FLIP. **(A)** Total lysates from PC12 cells (left panels) or cortical neurons maintained for 6 DIV (right panels) were treated or not with TNF-α and/or ActD for 24 h and analyzed by western blot using anti-TNF-R1, anti-TRADD, anti-FADD, anti-TRAF-2 and anti-RIP antibodies. Loading controls were performed by probing the membrane with an anti-panERK antibody. The optical density (OD) of the bands was scanned, and the ratio of the mean values was calculated with respect to the total protein content ($OD_{protein\ of\ interest}/OD_{panERK}$). These values are indicated in the upper part of the images for each protein and express the percentage of the protein in a given experimental condition with respect to the value of the untreated control ($Ratio_{condition}/Ratio_{control}$ x 100). **(B)** Total mRNA was extracted from PC12 cells (left panels) or cortical neurons maintained for 6 DIV (right panels) treated as in **(A)**. Semi-quantitative RT-PCR was performed for TNF-R2, caspase-8 and L27 (used as an internal control) transcripts. As a positive control for amplification, total mRNA isolated from post-natal rat liver was used. **(C-E)** Total cell lysates were obtained from PC12 cells after TNF-α and/or ActD time-course treatments and analyzed by western blot with the indicated antibodies. The optical density (OD) of the bands was scanned as in **(A)**. Detailed time-course analysis of $FLIP_L$ and $FLIP_S$ **(C)**, cIAP1 and cIAP2 **(D)** and XIAP **(E)** protein levels after treating PC12 cells as indicated. Equal loading was determined by probing the membrane with an anti-panERK antibody. **(F)** PC12 cells were infected with lentiviral particles carrying a hairpin with a scrambled sequence (Scr) or two different shRNA sequences targeting c-FLIP (F.1 and F.2), XIAP (X.1 and X.2) or cIAP2 (I2.1 and I2.2). At 3 days post-infection, cells were treated with 100 ng/ml TNF-α for 24 h or left untreated. Protein lysates were obtained as in **(A)**, and western blots against the different targeted proteins were performed, demonstrating the efficacy of the knock-downs (upper panel). In parallel, cell death was assessed by Hoechst 33258 staining (lower histogram).

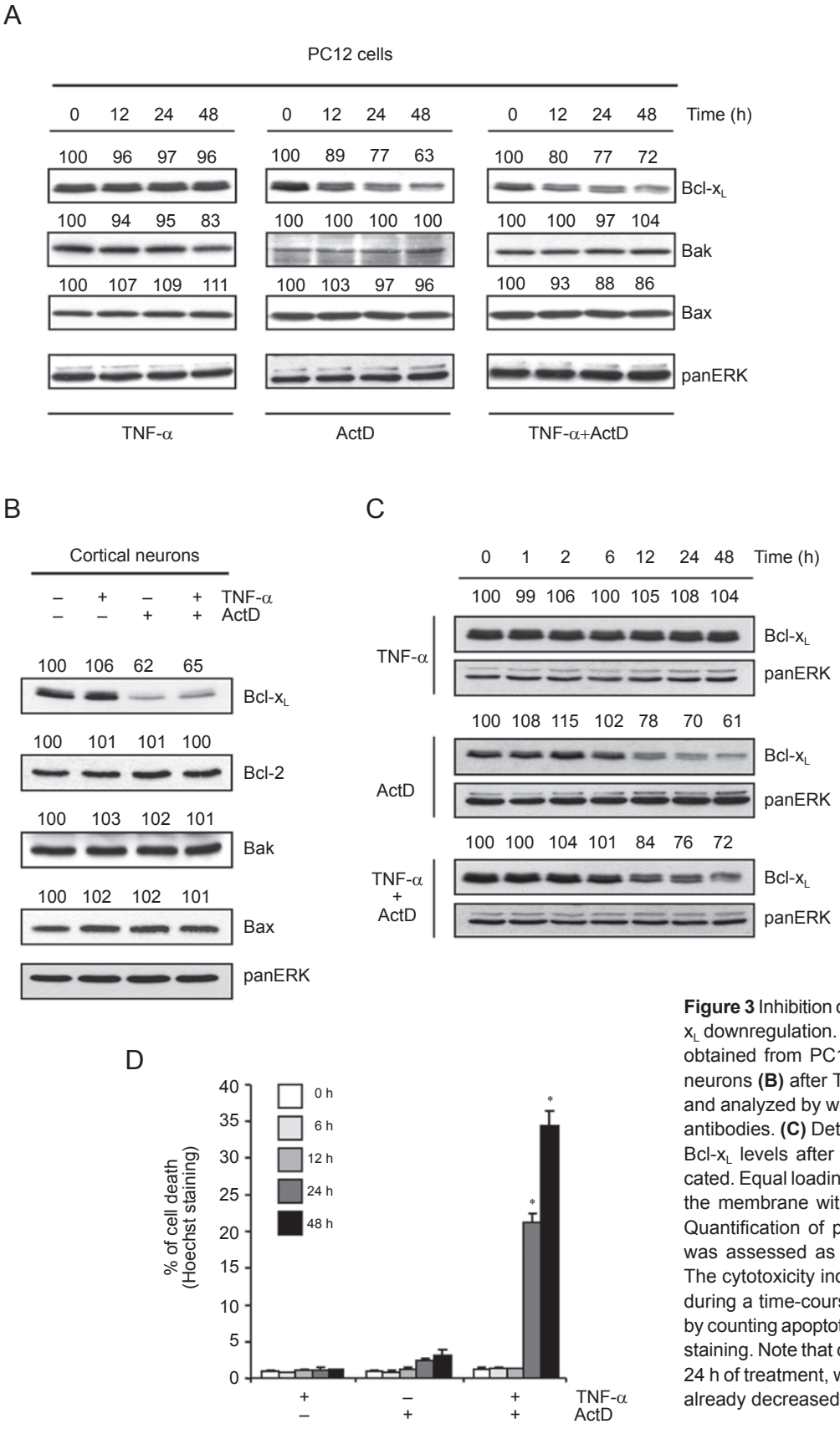

Figure 3 Inhibition of RNA synthesis induces Bcl-x_L downregulation. **(A, B)** Total cell lysates were obtained from PC12 cells **(A)** or DIV6 cortical neurons **(B)** after TNF-α and/or ActD treatment and analyzed by western blot with the indicated antibodies. **(C)** Detailed time-course analysis of Bcl-x_L levels after treating PC12 cells as indicated. Equal loading was determined by probing the membrane with an anti-panERK antibody. Quantification of protein in the different lanes was assessed as indicated in Figure 2A. **(D)** The cytotoxicity induced by TNF-α and/or ActD during a time-course up to 48 h was quantified by counting apoptotic nuclei after Hoechst 33258 staining. Note that cell death is only evident after 24 h of treatment, when the levels of Bcl-x_L have already decreased. *P < 0.01.

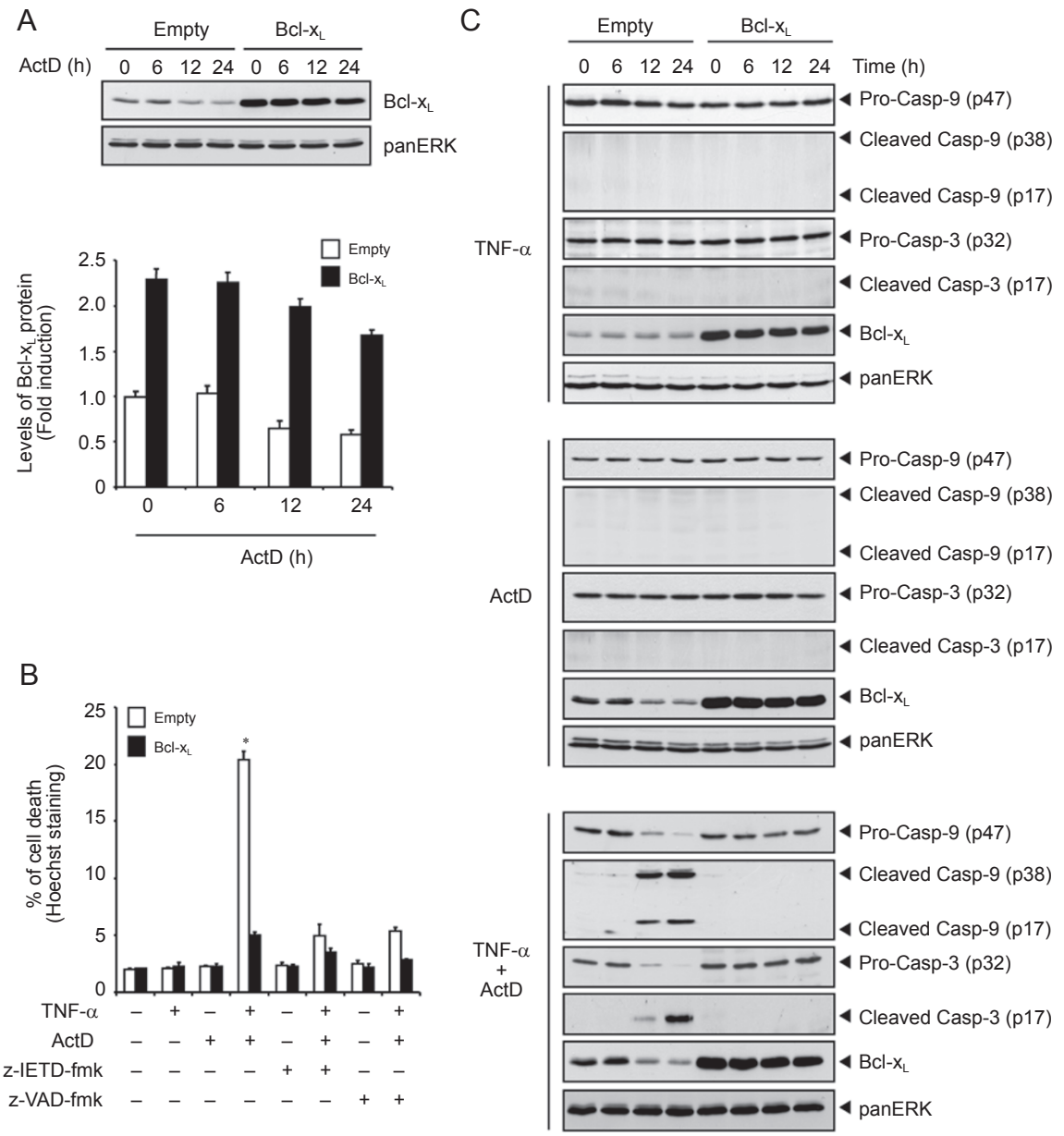

Figure 4 Transient Bcl-x_L overexpression prevents TNF-α/ActD-induced apoptosis in PC12 cells. **(A)** PC12 cells were infected with lentivirus containing a Bcl-x_L construct or an empty construct and were left in culture for 72 h to allow for transgene expression. Cells were then treated with ActD for the indicated times and the expression of Bcl-x_L was analyzed in total cell lysates by western blot using an anti-Bcl-x_L antibody. Total ERK (panERK) was used as loading control. The lower graph shows the quantitative analysis of Bcl-x_L expression levels in three independent experiments as described above. Fold induction is compared to empty-infected PC12 cells. **(B)** Cells were left untreated or treated for 24 h with TNF-α and/or ActD, and 50 μM z-IETD-fmk or 50 μM z-VAD.fmk was added when indicated. Cell death was quantified by counting apoptotic nuclei after Hoechst 33258 staining. **(C)** Bcl-x_L overexpression inhibits caspase activation induced by TNF-α/ActD treatment as assessed by detecting caspase-9 and caspase-3 active fragments. Anti-panERK antibody was used to confirm equal protein loading. **P* < 0.01.

ficient as the caspase inhibitors z-IETD-fmk or z-VAD-fmk in preventing apoptosis (Figure 4B). Protection against cell death in PC12-Bcl-x_L cells correlated with the inhibition of caspase-3 and -9 processing (Figure 4C).

When similar analyses were performed using cortical neurons, the results were comparable to those obtained for PC12 cells. Cortical neurons were infected with lentivirus carrying the construct expressing human Bcl-x_L at the

beginning of the culturing process and were cultured for 6 days. They were then treated with TNF-α, and cell death was assessed 24 h later by counting apoptotic nuclei using Hoechst staining. Increased Bcl-x_L expression completely prevented death induced by simultaneous treatment with TNF-α and ActD (Figure 5A). Bcl-x_L overexpression also prevented caspase activation as assessed by western blot analysis (Figure 5B), by measuring IETDase and DEVDase activities (Figure 5C and 5D) or by immunostaining for the active form of caspase-3 (Figure 5E).

Decreased endogenous Bcl-x_L levels render PC12 cells and cortical neurons sensitive to TNF-α without affecting NF-κB activity

To further assess the relevance of Bcl-x_L in resistance against TNF-α-mediated cytotoxicity, we carried out lentiviral-based knock-down of Bcl-x_L. As shown in Figure 6A, PC12 cells infected with lentivirus carrying a short hairpin sequence targeting rat/mouse Bcl-x_L (shBcl-x_L) exhibited a strong reduction in Bcl-x_L protein levels 72 h after infection when compared with cells infected by lentivirus carrying a scrambled sequence (shScr). PC12 cells infected with shScr or shBcl-x_L were treated with TNF-α/ActD, TNF-α or ActD alone for 24 h. As expected, cells containing the scrambled sequence only died when they were co-treated with TNF-α and ActD. Interestingly, PC12 cells infected with the shBcl-x_L construct were sensitive to the pro-apoptotic activity of TNF-α alone, and additional treatment with ActD did not further increase the number of apoptotic nuclei (Figure 6B). To confirm the specificity of the RNAi against Bcl-x_L and to rule out the possibility that non-specific targets could be responsible for mediating the sensitization of PC12 cells to TNF-α triggering, we carried out complementation experiments (Figure 6C). As shown in Figure 6D, infection with shBcl-x_L did not sensitize PC12 cells stably expressing human Bcl-x_L (PC12-hBcl-x_L) to TNF-α cell death. Figure 6E demonstrates that the shBcl-x_L lentivirus efficiently reduced Bcl-x_L levels in PC12 cells transfected with an empty (Neo) vector but not in PC12-hBcl-x_L cells. Moreover, Figure 6E shows that shBcl-x_L was efficient in reducing the levels of rat *bcl-x* mRNA, but not that of human *bcl-x* mRNA. These data confirm the specificity of this RNAi technology since the rat/mouse shBcl-x_L target sequence and the orthologous human sequence (GeneBank™ NM_138578) only differ by 3 nucleotides (Figure 6C).

To determine whether low levels of Bcl-x_L sensitize PC12 cells to TNF-α-induced cell death through the intrinsic apoptotic pathway, we assessed the activation of caspase-9 and caspase-3. PC12 cells transiently infected with shBcl-x_L and treated with TNF-α were able to process and activate pro-caspase-9 and pro-caspase-3 (Figure 7A). In contrast, shScr-infected PC12 cells were unable to activate these caspases (Figure 7A). In agreement with these results, TNF-α induced DEVD-like activity in shBcl-x_L-infected cells (Figure 7B). This activity can be completely rescued when cells were pre-treated with the caspase-8 inhibitor z-IETD-fmk (Figure 7B). Treatment with z-IETD-fmk or z-VAD-fmk also protected shBcl-x_L-infected cells from TNF-α-induced apoptosis (Figure 7C). We also carried out similar knock-down experiments in isolated mouse cortical neurons to confirm that Bcl-x_L is the key molecule that mediates resistance to TNF-α-mediated cytotoxicity. As shown in Figure 7D, lentivirus carrying the shBcl-x_L construct was highly efficient in knocking down endogenous Bcl-x_L protein levels in cortical neurons when compared with the scrambled sequence. Additionally, cortical neurons infected with shBcl-x_L became sensitive to TNF-α, showing a 5-fold increase in the number of apoptotic cells when compared with shScr-infected neurons (Figure 7E). Cell death induced by TNF-α in cortical neurons containing shBcl-x_L could be blocked by z-IETD-fmk (Figure 7E), demonstrating the involvement of a caspase-8-like activity. Pro-caspase-9 and pro-caspase-3 processing in TNF-α-treated cells was detected (Figure 7D), providing further evidence for the involvement of caspase-9 and caspase-3. Caspase-3 activation was also detected by measuring DEVDase activity (Figure 7F). Together, these results suggest that Bcl-x_L is the key molecule preventing TNF-α-induced apoptotic cell death in cortical neurons.

The NF-κB transcription factor has been postulated to be the key molecule mediating the anti-apoptotic response triggered by activation of TNF-R1. Indeed, it has been reported that disruption of the NF-κB pathway sensitizes cells to TNF-α-induced apoptosis [10, 11]. Because the downregulation of Bcl-x_L sensitized PC12 cells to TNF-α, we wanted to assess whether this effect was due to changes in NF-κB activation status. As shown in Figure 8A, knock-down of Bcl-x_L did not impair the ability of TNF-α to induce nuclear translocation of RelA/p65, and NF-κB activity was not altered by shBcl-x_L (Figure 8B). We also wanted to confirm that endogenous NF-κB function was not impaired in shBcl-x_L-PC12 cells treated with TNF-α. For this reason, we assessed the protein levels of cIAP1, a known target gene of NF-κB. As shown in Figure 8C, Bcl-x_L knock-down did not impair cIAP1 upregulation upon TNF-α treatment. In addition, blocking NF-κB activity via transfection of an IκBα super-repressor (SR-IκBα) (Figure 8D) [24] did not alter Bcl-x_L expression levels upon TNF-α treatment (Figure 8E), even though cell death occurred efficiently (Figure 8F). Altogether, our results point toward two different mechanisms that regulate cell sensitivity to apoptosis upon TNF-α treatment: one controlled by NF-κB status and the other controlled by Bcl-x_L protein levels.

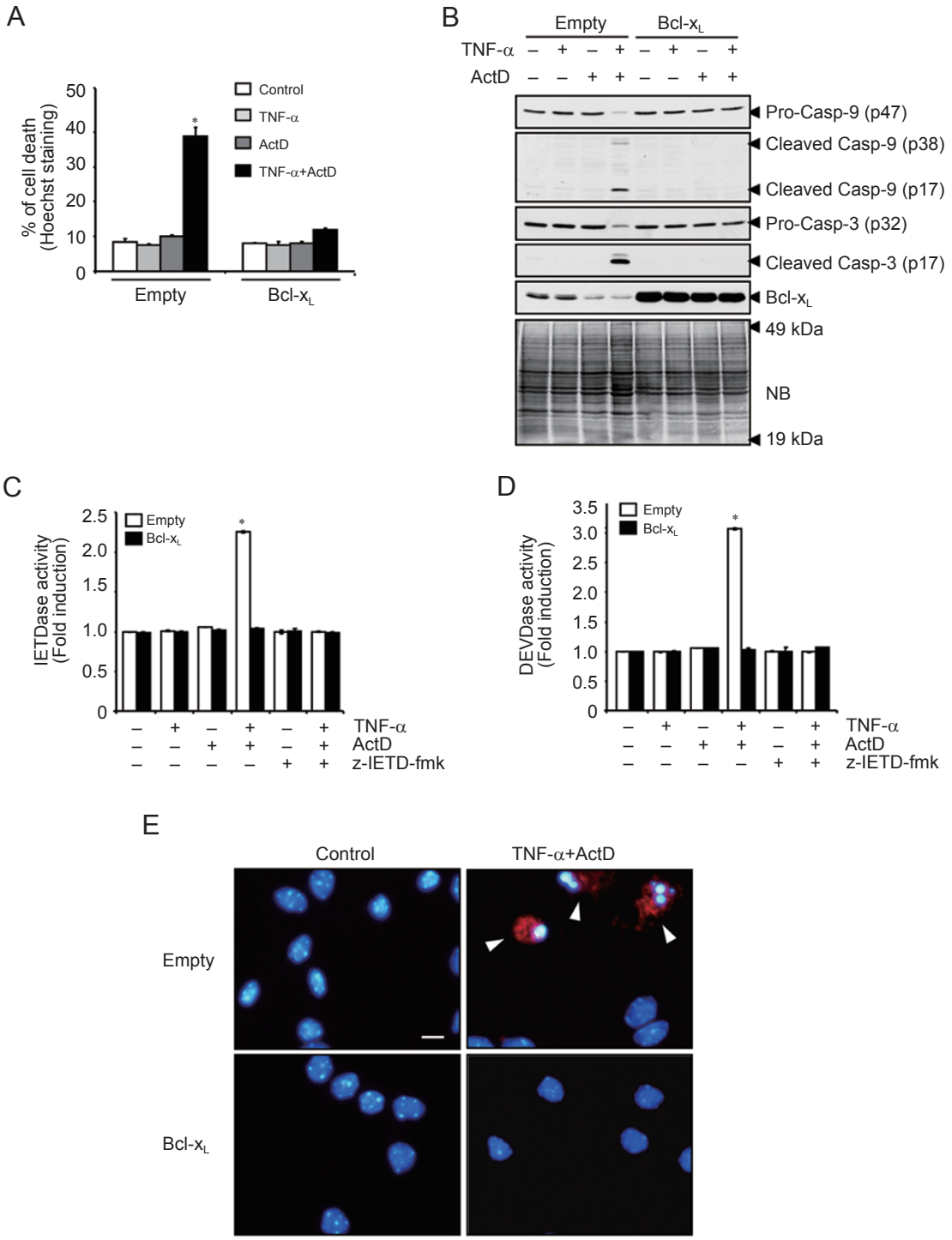

Figure 5 Transient Bcl-x_L overexpression prevents TNF-α/ActD-induced apoptosis in primary mouse cortical neurons. **(A)** Cortical neurons were infected with lentivirus containing a Bcl-x_L construct or an empty construct upon isolation. Cells were cultured for 6 days and treated for 24 h as indicated. Cell death was assessed by counting apoptotic nuclei after Hoechst 33258 staining. **(B)** Caspase-9 and -3 activities were analyzed by western blot using specific antibodies. Bcl-x_L overexpression was demonstrated by reprobing the membrane with a specific antibody. A loading control was performed by staining the membrane with Naphtol blue (NB). **(C**, **D)** Caspase-8-like **(C)** and caspase-3-like **(D)** activities in cortical neurons infected with a Bcl-x_L construct or an empty construct for 6 days were measured using fluorogenic Ac-IETD-afc or Ac-DEVD-afc reagents, respectively, after 8 h of the indicated treatments. Specificity was assessed by adding 50 μM of the caspase-8 inhibitor z-IETD-fmk during treatment. **(E)** Representative pictures show active caspase-3 immunofluorescence (red, arrows) merged with Hoechst 33258 nuclear staining. Bar represents 10 μm. *P < 0.01.

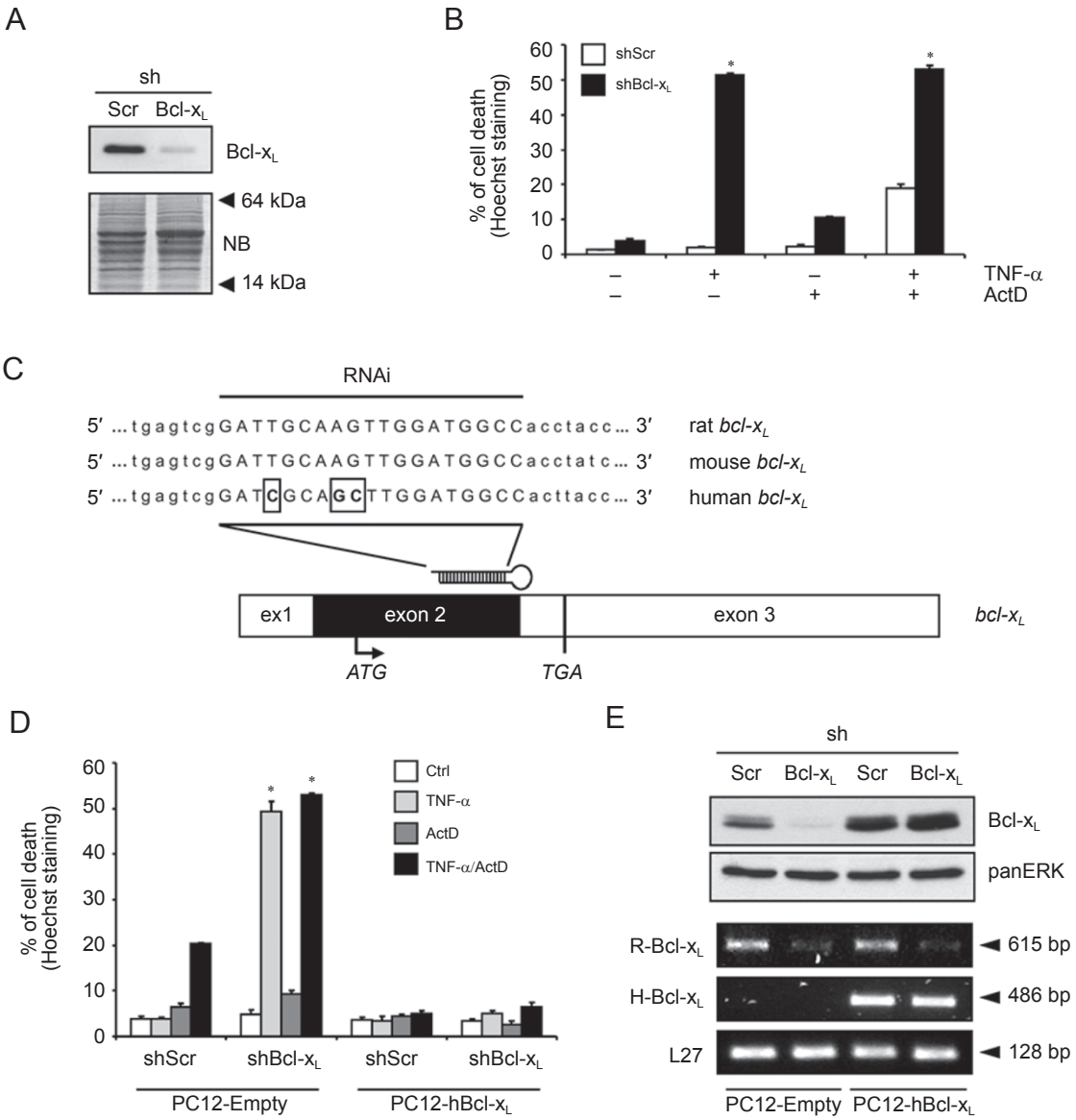

Figure 6 Bcl-x_L knock-down sensitizes PC12 cells to TNF-α-induced cell death. PC12 cells were infected with lentiviral particles containing an shRNA sequence targeting mouse/rat Bcl-x_L (shBcl-x_L) or a scrambled sequence as a control (shScr) for 3 days. **(A)** Bcl-x_L expression was analyzed in total lysates by western blot using anti-Bcl-x_L antibody. The membrane was stained with Naphtol blue (NB) to assess equal loading. **(B)** PC12 cells were infected for 3 days with shScr (white columns) or shBcl-x_L (black columns) and treated or not with 100 ng/ml TNF-α and/or 1 nM ActD for an additional 24 h. Cell death was quantified by counting apoptotic nuclei after Hoechst 33258 staining. **(C-E)** Complementation experiments demonstrate the specificity of Bcl-x_L knock-down by shRNA. PC12 cells stably transfected with an empty pcDNA3 plasmid (PC12-Neo) or a pcDNA3 plasmid containing the human Bcl-x_L (PC12-hBcl-x_L) were infected with lentivirus carrying shScr or shBcl-x_L. **(C)** Schematic diagram showing the coding sequences of rat, mouse and human *bcl-x*$_L$. shBcl-x_L targeted the mouse/rat sequence pictured as underlined and in capital letters. Differences in sequence are indicated by bold and boxed letters. **(D)** PC12 cells were left untreated (white bars), treated with TNF-α (light gray bars), ActD (deep gray bars) or with TNF-α/ActD (black bars) for 24 h. Cell death was measured by counting apoptotic nuclei after Hoechst staining. **(E)** (*Upper panel*) Protein lysates were taken from untreated PC12-Neo or PC12-hBcl-x_L cells that were previously infected for 3 days with shScr or shBcl-x_L virus as indicated. Total Bcl-x_L levels were analyzed by western blot, confirming Bcl-x_L knock-down in PC12-Neo cells. (*Lower panel*) Total mRNA was extracted under the same conditions described for the *upper panel*. RT-PCR for rat bcl-x_L (R-bcl-x_L, 615 bp amplification band), human bcl-x_L (H-bcl-x_L, 486 bp amplification band) or the housekeeping L27 mRNA (as a control of mRNA loading and amplification, 128 bp band) was performed. Note that shBcl-x_L was able to efficiently and specifically reduce rat bcl-x_L, but not human over-expressed bcl-x_L. *P < 0.01.

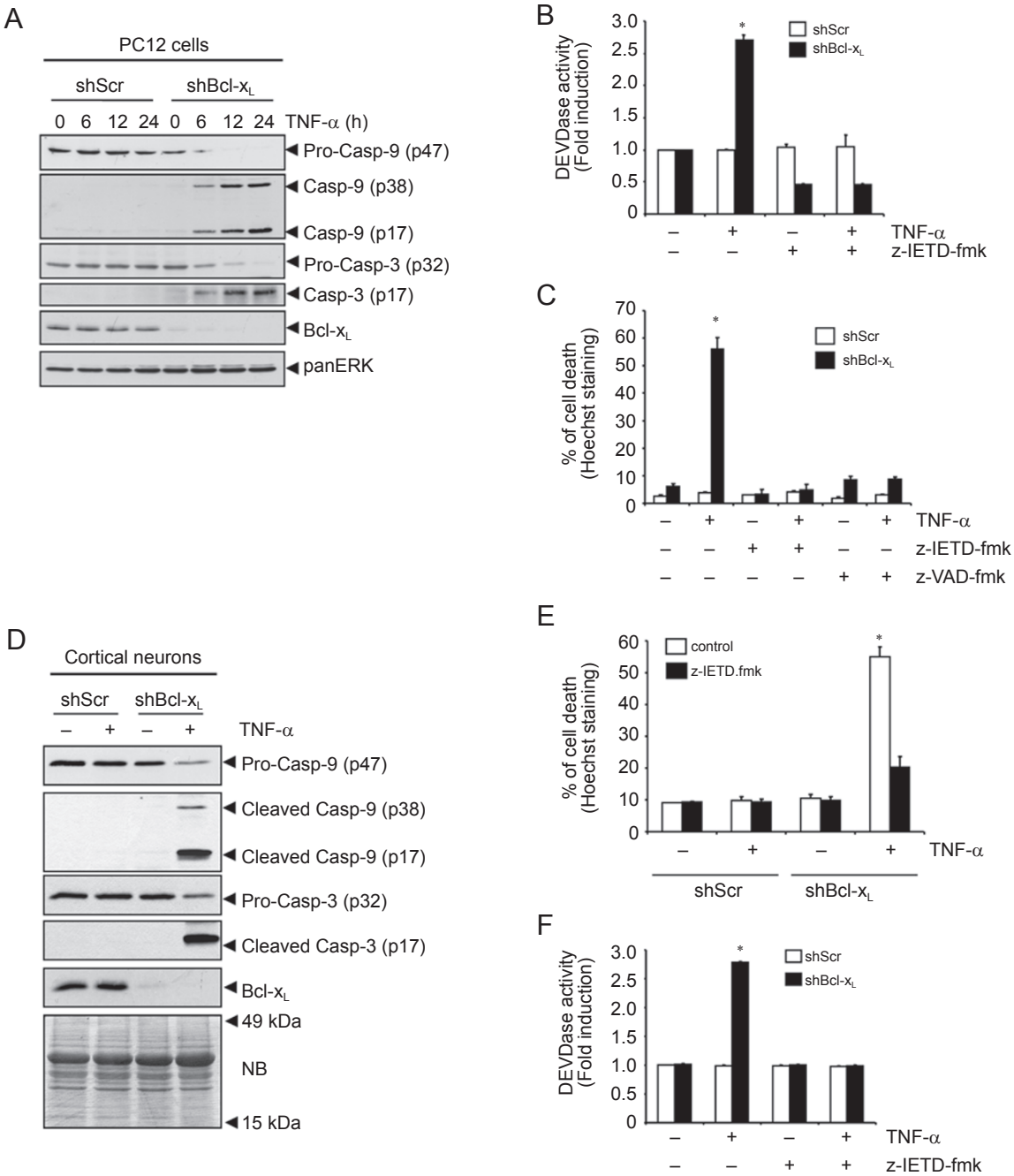

Figure 7 Bcl-x_L knock-down allows TNF-α to activate intracellular apoptotic signaling in PC12 cells and primary mouse cortical neurons. **(A-C)** Experiments performed in PC12 cells. **(D-F)** Experiments performed in isolated primary cortical neurons. **(A)** PC12 cells were treated or not with TNF-α, and caspase activation was detected over the indicated time-course by analyzing the appearance of caspase-9 or caspase-3 specific active fragments. pan-ERK reprobing of the membrane was used as a loading control. **(B)** Caspase-3-like activity was measured using the fluorogenic Ac-DEVD-afc reagent in cells after 8 h of treatment. **(C)** Cell death in cultures treated for 24 h in the presence of TNF-α and/or 50 μM z-IETD-fmk or 50 μM z-VAD-fmk, as indicated. Cell death was quantified by counting apoptotic nuclei after Hoechst 33258 staining. **(D)** Mouse cortical neurons were infected as described in Materials and Methods and cultured for 6 DIV. Cells were treated (+) or not (–) with TNF-α, and caspase-9 and -3 activation was assessed. Bcl-x_L knock-down after shBcl-x_L lentivirus infection was evident after reblotting of the membrane with an anti-Bcl-x_L antibody. The membrane was stained with Naphtol Blue (NB) to control for protein loading. **(E)** Cortical neurons cultured as described in **(D)** were treated with TNF-α and/or with 50 μM z-IETD-fmk for 24 h. Cell death was quantified by Hoechst 33258 nuclear staining. **(F)** Caspase-3-like activity was measured in the different experimental conditions indicated after 8 h of treatment using Ac-DEVD-afc. *P < 0.01.

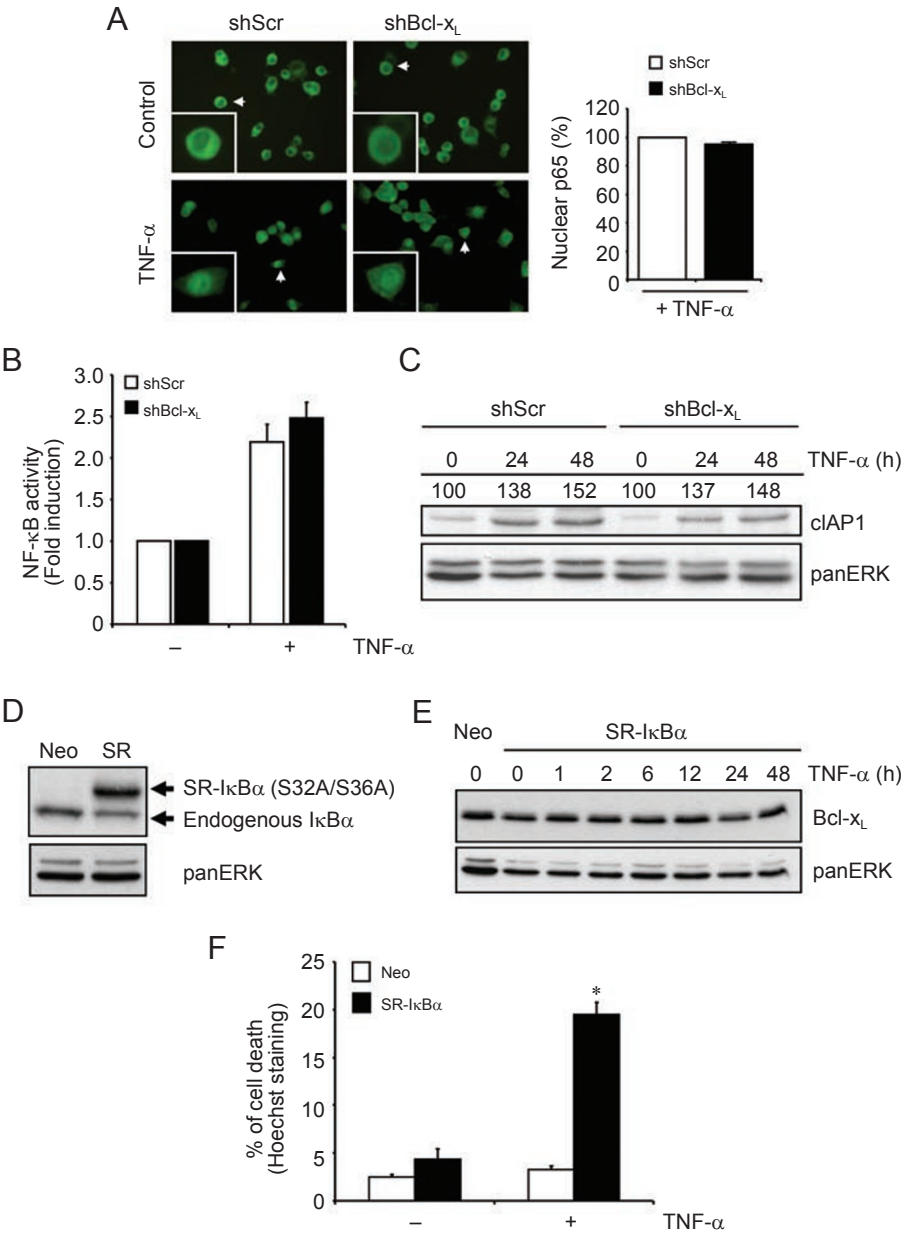

Figure 8 Bcl-x_L knock-down sensitizes cells to TNF-α-induced cell death without affecting NF-κB activity. **(A)** PC12 cells were transduced with shScr or shBcl-x_L lentivirus, and 3 days post-infection cells were left untreated (Ctrl) or treated with TNF-α for 6 h. Immunocytochemistry was performed to detect the p65 subunit of NF-κB. Representative low- and high-magnification photomicrographs are shown. (Arrowheads indicate the selected cells illustrated in the insets (high-magnification photomicrographs).) *Right*, a graph showing the percentage of nuclear p65 staining after TNF-α treatment of shScr- or shBcl-x_L-infected cells. Means ± SEM of three independent experiments are shown. **(B)** PC12 cells were transduced with shScr or shBcl-x_L lentivirus. At 3 days post-infection, cells were transiently transfected with an NF-κB-dependent reporter vector. After 24 h, the cells were treated with TNF-α for 6 h and luciferase activity was measured in the cell lysates using a Luciferase Assay System as described in Materials and Methods. **(C)** PC12 cells were transduced with shScr or shBcl-x_L lentivirus, and 3 days post-infection cells were left untreated (Ctrl) or treated with 100 ng/ml TNF-α for 24 and 48 h. Total cell lysates were obtained and analyzed by western blot using an antibody against cIAP1. Membranes were stripped and reprobed with an antibody against pan-ERK as a loading control. **(D)** PC12 cells were stably transfected with empty vector (Neo) or with SR-IκBα (SR-IκBα). Total cell lysates were analyzed by western blot using an antibody against IκBα. Membranes were stripped and reprobed with an antibody against pan-ERK as a loading control. **(E, F)** Lysates from untreated empty vector (Neo) or SR-IκBα-overexpressing PC12 cells treated with 100 ng/ml TNF-α at the times indicated were probed with an antibody against Bcl-x_L. Anti-panERK antibody was used to confirm equal protein loading. Apoptotic cell death was assessed after treatment with 100 ng/ml TNF-α for 24 h by Hoechst nuclear staining **(F)**. *$P < 0.01$.

Discussion

Cells treated with TNF-α usually require the inhibition of macromolecular synthesis in order to undergo apoptotic cell death [15, 25]. When metabolic inhibitors such as ActD are present in combination with TNF-α, caspase-8 becomes activated and induces apoptotic cell death. To explain this sensitizing effect, the inhibition of the synthesis of short-lived repressors of TNFR function has been widely postulated [25]. We demonstrate here that ActD renders PC12 cells and primary mouse cortical neurons susceptible to the cytotoxic effects of TNF-α, indicating that an initial sensitization step is required. We have also found that the intracellular levels of Bcl-x_L, and not those of FLIP or IAPs, determine resistance or sensitivity to TNF-α-triggered cell death, both in cortical neurons and in PC12 cells.

Two different types of intracellular pathways are activated by TNFRs: one promoting cell death and the other involved in cell survival. The pathways leading to cell survival mainly depend on NF-κB activation [11]. NF-κB controls the transcription of several genes that have been implicated in the inhibition of cell death via the TNF-α-mediated pro-apoptotic signaling pathway. Inhibition of NF-κB transcriptional activity allows for the induction of cell death by TNF-α [10, 11]. We demonstrate here that the specific reduction of Bcl-x_L protein levels renders cells sensitive to TNF-α-induced apoptosis. We provide evidence that NF-κB is fully functional in our system after TNF-α treatment despite reduced Bcl-x_L protein levels. Indeed, TNF-α can induce apoptosis when Bcl-x_L levels are reduced, even though NF-κB remains active. Therefore, the presence or absence of Bcl-x_L is critical for the decision of a cell whether to survive or die after exposure to TNF-α. Additionally, we found that when NF-κB activity is specifically inhibited by overexpression of a non-degradable form of IκB-α cells become sensitive to TNF-α-induced cell death without altering Bcl-x_L levels, suggesting that Bcl-x_L is not a target gene of the NF-κB pathway (Figure 8E). These data strongly support the idea that at least two different pro-survival signals co-exist in the TNF-α/TNFR signaling pathway, one of which is NF-κB-dependent and the other of which is NF-κB-independent but depends on Bcl-x_L levels.

It has been reported that the sensitization of some cell types to TNF-α-induced, NF-κB-dependent cell death is due to the degradation of c-$FLIP_L$ [26]. However, c-$FLIP_L$ protein levels did not decrease after ActD treatment in our cellular models. In addition, lentivirus-based knock-down of FLIP did not render cells sensitive to the pro-apoptotic action of TNF-α. It has also recently been suggested that TNF-α-dependent IAP upregulation could protect endothelial cells against the pro-apoptotic action of TNF-α [22, 27]. Our results demonstrate that TNF-α significantly upregulates and that ActD decreases c-IAP-1 and -2 protein levels. However, the cytotoxic combination of TNF-α and ActD did not modify the levels of these proteins as compared to untreated control cells. This finding implies that ActD impedes *de novo* TNF-α-mediated c-IAPs transcription, raising the hypothesis that the amount of c-IAPs present under these conditions could be insufficient to protect cells against TNF-α-triggered apoptosis. Nevertheless, the specific knock-down of c-IAP-1 (Supplementary information, Figure S1) or c-IAP-2 did not confer sensitivity to apoptosis induced by TNF-α treatment. Similarly, even though XIAP protein levels decreased upon ActD and TNF-α/ActD treatment, knock-down of XIAP did not confer sensitivity to TNF-α-mediated apoptosis. These data strongly indicate that neither FLIP nor IAPs are the key regulators of sensitization to TNF-α-mediated cell death, at least in our cellular models.

It has been recently shown that small molecules mimicking Smac/Diablo antagonism towards IAPs potentiate, or even induce, cell death in multiple cancer cell lines [28-30]. Regarding resistance or sensitivity to Smac/Diablo mimetics, we can expect three different classes of cancer cells. The first class is sensitive to Smac/Diablo mimetics. The second one does not respond to Smac/Diablo treatment alone, but becomes sensitive to TNF-α-induced apoptosis with this treatment. Finally, the third class may represent cancer cells that are resistant to Smac/Diablo mimetics and TNF-α co-treatment [31]. Intriguingly, cIAP degradation occurs regardless of the type of cancer cell or of sensitivity to Smac/Diablo mimetics upon mimetic treatment [29]. These data suggest that there should be other cIAP-independent mechanisms controlling the switch between cell survival and cell death in the TNF-α signaling cascade. Our data point to the mitochondria, and more specifically to Bcl-x_L protein levels, as an additional control in this pathway. In any case, it would be worthwhile to address the impact of Smac/Diablo mimetics on neuronal sensitivity to TNF-α.

A relevant finding reported here is that Bcl-2 protein levels remain unchanged after ActD treatment in cortical neurons. Although the functions of Bcl-2 family proteins appear similar, increasing evidence suggests that the pro-survival activities of Bcl-2 and Bcl-x_L are differentially regulated. In this sense, Bcl-2-inhibitable steps can normally be bypassed by the death receptor-mediated apoptotic pathway [32]. In contrast, Bcl-x_L is thought to be a more potent suppressor of death receptor-induced cell death [33]. Our results demonstrate that only Bcl-x_L levels were efficiently lowered by ActD treatment in cortical neurons, suggesting that Bcl-x_L protein, but not Bcl-2, must be degraded to make cells susceptible to TNF-α's pro-apoptotic

activity. In agreement with this, knock-down of Bcl-x_L in cortical neurons is an efficient way to induce TNF-α-mediated cell death. In fact, it has been reported that after nerve trauma Bcl-x_L expression is lost in axotomized neurons of the spinal ganglia [34]. Since TNF-α levels are drastically increased by resident activated glia in brain tissue after different pathological stimuli such as neural injury, ischemia or infection [2], we hypothesize that neurons with low Bcl-x_L levels become more sensitive to the cytotoxic activity of glial-derived TNF-α.

The physiological relevance of Bcl-x_L in the nervous system has been demonstrated by the generation of knock-out mice for *bcl-x*. In fact, the genetic ablation of *bcl-x* revealed that embryos die around day 13-13.5 due, in part, to extensive apoptotic cell death as evidenced in postmitotic immature neurons of the developing brain, spinal cord and dorsal root ganglia. These results confirm that Bcl-x supports the viability of immature cells during the embryonic development of the nervous system [35]. Moreover, no major alterations in the CNS were found in *bcl-2* knock-out mice, although some populations of neurons in the PNS were partially reduced [36, 37]. Our study demonstrates for the first time that Bcl-x_L, but not Bcl-2, is the key element in the resistance of primary neurons to TNF-α-triggered apoptosis.

Bcl-x_L expression is maintained or even upregulated during the development of the nervous system and in adulthood. However, Bcl-2 becomes quickly downregulated in almost every neuronal population during development [38-40]. Since Bax expression is also maintained in mature neurons [41], our data support the idea that the Bcl-x_L/Bax ratio might be one of the most important regulators of the response of neurons to TNF-α [40].

Materials and Methods

Reagents

All chemicals were obtained from Sigma-Aldrich (St Louis, MO) unless otherwise indicated. Human TNF-α (Sigma) was used at 100 ng/ml and ActD was used at 1 nM. The caspase inhibitors z-IETD-fmk and z-VAD-fmk and the fluorogenic caspase substrates Ac-IETD-afc and Ac-DEVD-afc were from Calbiochem (San Diego, CA). Antibodies against Bcl-x_L, FADD, RIP and panERK were purchased from BD Biosciences (San Diego, CA). Bcl-2 antibody was from Neomarkers (Westinghouse Drive Fremont, CA). Antibodies against Bax, cleaved caspase-3, procaspase-9 and cleaved caspase-9 were from Cell Signaling Technology (Beverly, MA). The anti-Bak antibody was from Biocarta (San Diego, CA). Antibodies against cIAP1, cIAP2, TNF-R1, TRAF-2 and TRADD were from Santa Cruz Biotechnology (Santa Cruz, CA). Antibodies against $FLIP_L$ and XIAP were from Stressgen (Ann Arbor, MI). The anti-$FLIP_S$ antibody was from Alexis (Lausen, Switzerland). The anti-Bid antibody was from R&D Systems (Benicia, CA).

Cell culture

PC12 cells were cultured in Dulbecco's modified Eagle's medium (DMEM) supplemented with 6% heat-inactivated fetal bovine serum (FBS), 6% heat-inactivated horse serum (Gibco Invitrogen Corp., Paisley, UK), 10 mM HEPES, 20 units/ml penicillin and 20 μg/ml streptomycin. Primary cortical neurons were dissected from E15 mouse embryos into ice-cold HBSS (Invitrogen), trypsinized for 8 min at 37 ºC and dissociated with a fire-polished Pasteur pipette. The resulting cells were plated at 7.5×10^4 cells/cm^2 in 10 μg/ml poly-D-lysine-coated culture plates and cultured in MEM supplemented with 10% FBS for 4 h. The medium was then replaced with serum-free MEM supplemented with B27 and N2 (Gibco), and neurons were maintained for 6 days *in vitro* (DIV) before treatment. Cultures were maintained at 37 ºC in a humidified atmosphere of 95% air and 5% CO_2.

Plasmids

For transient overexpression, the cDNA for human Bcl-x_L was extracted from pcDNA3 (Invitrogen) [42] and subcloned into pWPI [43, 44]. PC12 cells stably transfected with IκBα super-repressor (SR-IκBα)-pcDNA3 or empty-pcDNA3 vectors were obtained as described by Sole *et al*. [45]. For RNAi experiments, constructs were generated in pSUPER.retro.puro (OligoEngine, Seattle, WA) using specific oligonucleotides targeting Bcl-x_L, c-FLIP or cIAP2 sequences as follows: shBcl-x_L GAT TGC AAG TTG GAT GGC C; shFLIP-*F.1* GGT TCC GAT CAG TTG AAT T; shFLIP-*F.2* CAC CTT GTT TCC GAT TAT A; shXIAP-*X.1* AGA ATC CTA TGG TGC AAG A; shXIAP-*X.2* GGT GCA AGA AGC TAT ACG; shIAP2-*I2.1* CAC GGA GAA GGC CAG ATT A and shIAP2-*I2.2* GTT CGT TGG CCA AGT TCA A. The control scrambled (shScr) sequence was GGT CCC TTT CTC TGT AGT C. Adaptors to clone the oligonucleotides into the *Bgl*II/*Hind*III sites of pSUPER.retro.puro were added as required. Oligonucleotides were obtained from Sigma-Aldrich. Lentiviral constructs were generated by digesting pSUPER-sh with *Eco*RI and *Cla*I to replace the H1 promoter with the H1-shRNA cassette in pLVTHM. pWPI, pLVTHM, pSPAX2 and pMD2G were kindly provided by Dr Trono (Université de Genève, Geneva, Switzerland).

Production of lentiviral particles and cell transduction

Lentiviruses were propagated in HEK293T cells, using methods described previously [43, 44]. Using the calcium phosphate method [46], 20 μg of pLVTHM-Bcl-x_L, 13 μg of pSPAX2 and 7 μg of pM2G were transfected. Cells were allowed to produce lentivirus for 48 h. Then the medium was centrifuged at 1 200 × *g* for 5 min, and the supernatant was filtered using a 45 μm filter. Lentivirus was concentrated at 50 000 × *g* for 90 min and resuspended in 20 μl phosphate-buffered saline (PBS) containing 1% BSA. Lentiviruses were stored at –80 ºC. Biological titers of the viral preparations, expressed as the number of transducing units per ml (TU/ml), were determined by transducing HEK293T cells in limiting dilutions. After 48 h incubation, the percentage of GFP-positive cells was counted and viruses at 5×10^8–1×10^9 TU/ml were used in the experiments.

Lentiviral transduction experiments were carried out as described elsewhere [47]. Briefly, cells were seeded in 24-well plates at a density of 10^5 cells/well. Concentrated lentivirus (2 μl) was added (minimum MOI = 5). After 4 h, the medium was changed and infection efficiency was monitored in each experiment by direct counting of GFP-positive cells. The frequency of infection rose to 90% and 99% for cortical neurons and PC12 cells, respectively. A time-course

analysis was performed to test for efficient Bcl-x_L overexpression or knock-down. Bcl-x_L levels were assessed by western blot and, after 3 days of infection, viruses carrying Bcl-x_L or shBcl-x_L efficiently induced Bcl-x_L protein overexpression or reduced Bcl-x_L protein levels, respectively. Selection of pools of cells transfected with human Bcl-x_L or empty pcDNA3 [42] was performed by adding G-418 to the medium at a final concentration of 500 μg/ml (Gibco).

Western blots

Cells were rinsed in ice-cold PBS (pH 7.2) after stimulation. Cells were lysed with pre-warmed (95 ºC) 2% sodium dodecyl sulfate (SDS)-125 mM Tris (pH 6.8) and protein concentration was quantified using a modified Lowry assay (Bio-Rad Dc protein assay, Bio-Rad, Hercules, CA). Cell lysates (25 μg of protein) were separated on SDS/PAGE gels and transferred to a polyvinylidene difluoride (PVDF) Immobilon-P transfer membrane (Millipore, Bedford, MA). After blocking with Tris-buffered saline with Tween-20 containing 5% non-fat dry milk for 1 h at room temperature, the membranes were probed with the appropriated primary antibodies according to the specific requirements indicated by each provider. After 1 h of incubation with the specific peroxidase-conjugated secondary antibodies, the membranes were developed with the EZ-ECL chemiluminescence detection kit (Biological Industries, Kibbutz Beit Haemek, Israel).

Cell viability assays

Cells were seeded in 24-well plates at 5×10^4 cells/well, cultured for 24 h with complete growth medium and treated for the indicated times. Cell viability assays were performed as described previously [48, 49]. Briefly, for the Trypan Blue staining exclusion assay, cells were harvested and resuspended in 100 μl of PBS solution. Trypan Blue dye (20 μl; 0.08% final concentration) (Sigma) was added to the cell suspension. Cells were counted using a hemocytometer. For apoptotic nuclear morphology assessment, cells were fixed with 4% paraformaldehyde and stained with 0.05 μg/ml Hoechst 33258 for 30 min at room temperature. Uniformly stained nuclei were scored as healthy, viable cells, whereas condensed or fragmented nuclei were scored as dead cells (apoptotic nuclear morphology type II) [50]. Apoptosis was also assessed by TUNEL staining. Cells were fixed in 4% paraformaldehyde/PBS for 60 min at room temperature, permeabilized with 0.1% Triton X-100 in 0.1% sodium citrate for 2 min at 4 ºC, and processed following the *In situ Cell Death Detection Kit* instructions (Roche). At the final step, Hoechst 33258 was added at a final concentration of 0.05 μg/ml. Cell death was quantified using an Olympus microscope equipped with epifluorescence optics.

Caspase activity

After the indicated treatments, cells were rinsed once with PBS and resuspended in lysis buffer containing 25 mM HEPES/NaOH pH 7.5, 10 mM DTT, 5 mM EDTA, 5 mM $MgCl_2$ and 1 mM PMSF for the DEVD-directed activities (caspase-3-like) or 20 mM HEPES/NaOH pH 7.2, 150 mM NaCl, 10 mM DTT and 1 mM PMSF for IETD-like activities (caspase-8-like), both with 1% Triton-X-100. Lysates were cleared by centrifugation at 16 000 × *g* for 5 min and supernatant proteins were quantified by the Bradford method. Assays were performed using 25 μg of protein for caspase-3-like activities or 100 μg for caspase-8-like activities in the specific lysis buffer supplemented with 10% saccharose and 0.1% CHAPS plus 50 μM of the fluorogenic substrate Ac-DEVD-afc or 150 μM Ac-IETD-afc. Plates were read in a Bio-Tek FL 600 Fluorimeter (Izasa, Spain) using a 360 nm (40 nm bandwidth) excitation filter and a 530 nm (25 nm bandwidth) emission filter.

Active caspase-3 immunofluorescence

Cells were rinsed with PBS at room temperature and fixed in 4% paraformaldehyde/PBS for 30 min. They were then washed twice with PBS and permeabilized and blocked with 3% FBS and 0.1% Triton X-100 in PBS for 60 min. Cells were incubated overnight at 4 ºC with rabbit polyclonal anti-cleaved caspase-3 (Cell Signaling) diluted 1:150, rinsed three times with PBS, and incubated with Alexa Fluor 594-conjugated anti-rabbit secondary antibodies (Molecular Probes, Eugene, OR) diluted 1:250 for 1 h at room temperature and protected from light. Finally, cells were stained with 0.05 μg/ml Hoechst 33258 for 30 min [48]. Micrographs were obtained using an inverted Olympus XT microscope.

RT-PCR

Cells were treated as described above and mRNA was isolated with the RNeasy® kit according to the manufacturer's instructions (Qiagen, Valencia, CA). Using 150 ng of random hexamers for 1 h at 42 ºC, 1 μg of each sample was reverse transcribed by MMLV (Moloney Murine Leukemia Virus) Reverse Transcriptase. Approximately 10 ng of cDNA per sample was amplified by PCR in a Perkin-Elmer thermal cycler 2400 with 200 nM of each primer. The PCR conditions were 94 °C for 30 s, 60 °C for 30 s and 72 °C for 40 s for 28 cycles in 50 mM Tris-HCl pH 9.0, 2.5 mM $MgCl_2$, 15 mM $(NH_4)_2SO_4$, 0.1% Triton X-100 and 1 unit of DyNAzime-EXT DNA polymerase (Finnzymes, Espoo, Finland). Primers used were rBclX_F (5′-AGA GAG GCT GGC GAT GAG TTT GAA-3′) and rBclX1-2_R (5′-AGC AGA ACA CAG GGA GAA CTT GCT-3′), which amplify a band corresponding to part of the open reading frame (ORF) of rat Bcl-x_L (GenBank™ accession NM_001033672); hBclXL-S_F (5′-AGC TGG TGG TTG ACT TTC TCT CCT-3′) and hBclXL_R (5′-AAG CTG CGA TCC GAC TCA CCA ATA-3′), which cover a region containing a portion of the human Bcl-x_L ORF (GenBank™ accession NM_138578); rTNF-R2_F (5′-GGC TCA GAT GTG CTG TGC TA-3′) and rTNF-R2_R (5′-TGG TTC CAG ACC TGG GTA-3′), which amplify a band corresponding to part of the ORF of rat TNF-R2 (GenBank™ accession NM_130426); rCasp-8_F (5′-TGC CCT CAA GTT CCT GTG C-3′) and rCasp-8_R (5′-CTT CTG AGA GCT TAA AGA GCA TAA C-3′), which amplify a band corresponding to a part of the ORF of rat caspase-8 (GenBank™ accession NM_022277); and L27_F (5′-AGC TGT CAT CGT GAA GAA-3′) and L27_R (5′-CTT GGC GAT CTT CTT CTT GCC-3′) for the L27 house-keeping ribosomal protein.

Immunofluorescence of RelA/p65 nuclear translocation and NF-κB activity assay

To determine NF-κB status (RelA/p65 nuclear translocation and NF-κB activity) experiments were performed as described previously [45].

Statistical analysis

All experiments were performed at least three times. Values were expressed as means ± SEM. Student's *t*-tests were used to determine the statistical significance of differences in cell death and caspase activity values. $P < 0.01$ was considered to be significant.

Acknowledgments

We thank Dr Jose M Lizcano (Institut de Neurociències-UAB, Barcelona, Spain) for helpful discussions, and Arantzazu Rodriguez-Asiain (Institut de Neurociències-UAB, Barcelona, Spain), Isabel Sánchez-López and Roser Pané (Universitat de Lleida, Lleida, Spain) for technical assistance. We also thank Dr Trono (Genève, Switzerland) for providing the lentivirus plasmids. This work was funded by Spanish Government "Ministerio de Sanidad y Consumo" (Redes Temáticas de Investigación Cooperativa and CIBERNED), Spanish Government "Ministerio de Educación y Ciencia" (SAF2007-60287) and Generalitat de Catalunya (Suport als Grups de Recerca Consolidats) to JXC, and by grants from "Ministerio de Educación y Ciencia" SAF2005-05106 (to JR-A) and SAF2005-02197 (to DS). RG and VI-G hold postgraduate fellowships from the *DURSI* (*Generalitat de Catalunya*) *and Fons Social Europeu*. CS and MFS were supported by postgraduate fellowships from the Spanish Government, *MEC* and *FIS*, respectively. RSM is under a postdoctoral contract associated with the SAF2007-60287 grant. SR is supported by a postdoctoral contract from the CIBERNED. JZ holds a fellowship from "Ministerio de Educación y Ciencia". NB is a recipient of a fellowship from the "Gobierno Vasco". DS is under the *Ramon y Cajal* Program from the "Ministerio de Educación y Ciencia" (Spain). VJY was supported by a *Beatriu de Pinós* contract from *Generalitat de Catalunya* and is presently under the 2006 *Ramon y Cajal* Program from the "Ministerio de Educación y Ciencia" (Spain), co-financed by the European Social Fund.

References

1 Breder CD, Tsujimoto M, Terano Y, Scott DW, Saper CB. Distribution and characterization of tumor necrosis factor-alpha-like immunoreactivity in the murine central nervous system. *J Comp Neurol* 1993; **337**:543-567.
2 Perry VH, Tsao JW, Fearn S, Brown MC. Radiation-induced reductions in macrophage recruitment have only slight effects on myelin degeneration in sectioned peripheral nerves of mice. *Eur J Neurosci* 1995; **7**:271-280.
3 Raivich G, Liu ZQ, Kloss CU, *et al.* Cytotoxic potential of pro-inflammatory cytokines: combined deletion of TNF receptors TNFR1 and TNFR2 prevents motoneuron cell death after facial axotomy in adult mouse. *Exp Neurol* 2002; **178**:186-193.
4 Sriram K, Matheson JM, Benkovic SA, *et al.* Mice deficient in TNF receptors are protected against dopaminergic neurotoxicity: implications for Parkinson's disease. *Faseb J* 2002; **16**:1474-1476.
5 Sriram K, Matheson JM, Benkovic SA, *et al.* Deficiency of TNF receptors suppresses microglial activation and alters the susceptibility of brain regions to MPTP-induced neurotoxicity: role of TNF-alpha. *Faseb J* 2006; **20**:670-682.
6 Martin-Villalba A, Hahne M, Kleber S, *et al.* Therapeutic neutralization of CD95-ligand and TNF attenuates brain damage in stroke. *Cell Death Differ* 2001; **8**:679-686.
7 Demjen D, Klussmann S, Kleber S, *et al.* Neutralization of CD95 ligand promotes regeneration and functional recovery after spinal cord injury. *Nat Med* 2004; **10**:389-395.
8 Wajant H, Pfizenmaier K, Scheurich P. Tumor necrosis factor signaling. *Cell Death Differ* 2003; **10**:45-65.
9 Micheau O, Tschopp J. Induction of TNF receptor I-mediated apoptosis via two sequential signaling complexes. *Cell* 2003; **114**:181-190.
10 Beg AA, Baltimore D. An essential role for NF-kappaB in preventing TNF-alpha-induced cell death. *Science* 1996; **274**:782-784.
11 Van Antwerp DJ, Martin SJ, Kafri T, Green DR, Verma IM. Suppression of TNF-alpha-induced apoptosis by NF-kappaB. *Science* 1996; **274**:787-789.
12 Wang CY, Mayo MW, Baldwin Jr AS. TNF- and cancer therapy-induced apoptosis: potentiation by inhibition of NF-kappaB. *Science* 1996; **274**:784-787.
13 Martin SJ, Lennon SV, Bonham AM, Cotter TG. Induction of apoptosis (programmed cell death) in human leukemic HL-60 cells by inhibition of RNA or protein synthesis. *J Immunol* 1990; **145**:1859-1867.
14 Suzuki A, Tsutomi Y, Akahane K, Araki T, Miura M. Resistance to Fas-mediated apoptosis: activation of caspase 3 is regulated by cell cycle regulator p21WAF1 and IAP gene family ILP. *Oncogene* 1998; **17**:931-939.
15 Fulda S, Meyer E, Debatin KM. Metabolic inhibitors sensitize for CD95 (APO-1/Fas)-induced apoptosis by down-regulating Fas-associated death domain-like interleukin 1-converting enzyme inhibitory protein expression. *Cancer Res* 2000; **60**:3947-3956.
16 Chen C, Edelstein LC, Gelinas C. The Rel/NF-kappaB family directly activates expression of the apoptosis inhibitor Bcl-x(L). *Mol Cell Biol* 2000; **20**:2687-2695.
17 Sawada M, Nakashima S, Banno Y, *et al.* Influence of Bax or Bcl-2 overexpression on the ceramide-dependent apoptotic pathway in glioma cells. *Oncogene* 2000; **19**:3508-3520.
18 Deng Y, Lin Y, Wu X. TRAIL-induced apoptosis requires Bax-dependent mitochondrial release of Smac/DIABLO. *Genes Dev* 2002; **16**:33-45.
19 Clohessy JG, Zhuang J, de Boer J, Gil-Gomez G, Brady HJ. Mcl-1 interacts with truncated Bid and inhibits its induction of cytochrome c release and its role in receptor-mediated apoptosis. *J Biol Chem* 2006; **281**:5750-5759.
20 Mielke K, Herdegen T. Fatal shift of signal transduction is an integral part of neuronal differentiation: JNKs realize TNFalpha-mediated apoptosis in neuronlike, but not naive, PC12 cells. *Mol Cell Neurosci* 2002; **20**:211-224.
21 Sohn D, Totzke G, Essmann F, *et al.* The proteasome is required for rapid initiation of death receptor-induced apoptosis. *Mol Cell Biol* 2006; **26**:1967-1978.
22 Furusu A, Nakayama K, Xu Q, Konta T, Kitamura M. MAP kinase-dependent, NF-kappaB-independent regulation of inhibitor of apoptosis protein genes by TNF-alpha. *J Cell Physiol* 2007; **210**:703-710.
23 Vaux DL, Cory S, Adams JM. Bcl-2 gene promotes haemopoietic cell survival and cooperates with c-myc to immortalize pre-B cells. *Nature* 1988; **335**:440-442.

24 Rodriguez MS, Wright J, Thompson J, *et al.* Identification of lysine residues required for signal-induced ubiquitination and degradation of I kappa B-alpha *in vivo*. *Oncogene* 1996; **12**:2425-2435.
25 Kroemer G, Martinez C. Pharmacological inhibition of programmed lymphocyte death. *Immunol Today* 1994; **15**:235-242.
26 Chang L, Kamata H, Solinas G, *et al.* The E3 ubiquitin ligase itch couples JNK activation to TNFalpha-induced cell death by inducing c-FLIP(L) turnover. *Cell* 2006; **124**:601-613.
27 Deng Y, Ren X, Yang L, Lin Y, Wu X. A JNK-dependent pathway is required for TNFalpha-induced apoptosis. *Cell* 2003; **115**:61-70.
28 Petersen SL, Wang L, Yalcin-Chin A, *et al.* Autocrine TNFalpha signaling renders human cancer cells susceptible to Smac-mimetic-induced apoptosis. *Cancer Cell* 2007; **12**:445-456.
29 Varfolomeev E, Blankenship JW, Wayson SM, *et al.* IAP antagonists induce autoubiquitination of c-IAPs, NF-kappaB activation, and TNFalpha-dependent apoptosis. *Cell* 2007; **131**:669-681.
30 Vince JE, Wong WW, Khan N, *et al.* IAP antagonists target cIAP1 to induce TNFalpha-dependent apoptosis. *Cell* 2007; **131**:682-693.
31 Wu H, Tschopp J, Lin SC. Smac mimetics and TNFalpha: a dangerous liaison? *Cell* 2007; **131**:655-658.
32 Chao DT, Korsmeyer SJ. BCL-2 family: regulators of cell death. *Annu Rev Immunol* 1998; **16**:395-419.
33 Fernandez Y, Espana L, Manas S, Fabra A, Sierra A. Bcl-xL promotes metastasis of breast cancer cells by induction of cytokines resistance. *Cell Death Differ* 2000; **7**:350-359.
34 Chelyshev YA, Raginov IS, Guseva DS, Masgutov RF. Survival and phenotypic characteristics of axotomized neurons in spinal ganglia. *Neurosci Behav Physiol* 2005; **35**:457-460.
35 Motoyama N, Wang F, Roth KA, *et al.* Massive cell death of immature hematopoietic cells and neurons in Bcl-x-deficient mice. *Science* 1995; **267**:1506-1510.
36 Nakayama K, Nakayama K, Negishi I, *et al.* Disappearance of the lymphoid system in Bcl-2 homozygous mutant chimeric mice. *Science* 1993; **261**:1584-1588.
37 Veis DJ, Sorenson CM, Shutter JR, Korsmeyer SJ. Bcl-2-deficient mice demonstrate fulminant lymphoid apoptosis, polycystic kidneys, and hypopigmented hair. *Cell* 1993; **75**:229-240.
38 Gonzalez-Garcia M, Garcia I, Ding L, *et al.* bcl-x is expressed in embryonic and postnatal neural tissues and functions to prevent neuronal cell death. *Proc Natl Acad Sci USA* 1995; **92**:4304-4308.
39 Merry DE, Veis DJ, Hickey WF, Korsmeyer SJ. bcl-2 protein expression is widespread in the developing nervous system and retained in the adult PNS. *Development* 1994; **120**:301-311.
40 Parsadanian AS, Cheng Y, Keller-Peck CR, Holtzman DM, Snider WD. Bcl-xL is an antiapoptotic regulator for postnatal CNS neurons. *J Neurosci* 1998; **18**:1009-1019.
41 Krajewski S, Krajewska M, Shabaik A, *et al.* Immunohistochemical determination of *in vivo* distribution of Bax, a dominant inhibitor of Bcl-2. *Am J Pathol* 1994; **145**:1323-1336.
42 Yuste VJ, Bayascas JR, Llecha N, *et al.* The absence of oligonucleosomal DNA fragmentation during apoptosis of IMR-5 neuroblastoma cells: disappearance of the caspase-activated DNase. *J Biol Chem* 2001; **276**:22323-22331.
43 Naldini L, Blomer U, Gage FH, Trono D, Verma IM. Efficient transfer, integration, and sustained long-term expression of the transgene in adult rat brains injected with a lentiviral vector. *Proc Natl Acad Sci USA* 1996; **93**:11382-11388.
44 Zufferey R, Dull T, Mandel RJ, *et al.* Self-inactivating lentivirus vector for safe and efficient *in vivo* gene delivery. *J Virol* 1998; **72**:9873-9880.
45 Sole C, Dolcet X, Segura MF, *et al.* The death receptor antagonist FAIM promotes neurite outgrowth by a mechanism that depends on ERK and NF-kapp B signaling. *J Cell Biol* 2004; **167**:479-492.
46 Cullen BR. Use of eukaryotic expression technology in the functional analysis of cloned genes. *Methods Enzymol* 1987; **152**:684-704.
47 Segura MF, Sole C, Pascual M, *et al.* The long form of Fas apoptotic inhibitory molecule is expressed specifically in neurons and protects them against death receptor-triggered apoptosis. *J Neurosci* 2007; **27**:11228-11241.
48 Boix J, Llecha N, Yuste VJ, Comella JX. Characterization of the cell death process induced by staurosporine in human neuroblastoma cell lines. *Neuropharmacology* 1997; **36**:811-821.
49 Yuste VJ, Sanchez-Lopez I, Sole C, *et al.* The prevention of the staurosporine-induced apoptosis by Bcl-X(L), but not by Bcl-2 or caspase inhibitors, allows the extensive differentiation of human neuroblastoma cells. *J Neurochem* 2002; **80**:126-139.
50 Yuste VJ, Sanchez-Lopez I, Sole C, *et al.* The contribution of apoptosis-inducing factor, caspase-activated DNase, and inhibitor of caspase-activated DNase to the nuclear phenotype and DNA. *J Biol Chem* 2005; **280**:35670-35683.

(**Supplementary information** is linked to the online version of the paper on the Cell Research website.)